Airborne Doppler Wind Lidar Technology Demonstration for Aeolus – from Pre-launch Campaigns to Mission Performance Validation

Christian Lemmerz *[a], Oliver Lux [a], Benjamin Witschas [a], Stephan Rahm [a], Uwe Marksteiner [a], Alexander Geiß [b], Fabian Weiler [a], Oliver Reitebuch [a]
[a]German Aerospace Center (Deutsches Zentrum für Luft- und Raumfahrt e.V., DLR), Institute of Atmospheric Physics, Oberpfaffenhofen 82234, Germany; [b]Ludwig-Maximilians-University Munich, Meteorological Institute, 80333 Munich, Germany

ABSTRACT

In cooperation with the European Space Agency (ESA) and Airbus Defense and Space (DS), the German Aerospace Center (DLR) developed the ALADIN Airborne Demonstrator (A2D). Also operating at 355 nm wavelength, it is the prototype of the first direct-detection Doppler wind lidar instrument in space - ALADIN (Atmospheric Laser Doppler Instrument) - the single payload of ESA's Aeolus mission. The A2D was deployed for extensive ground-based measurements and airborne campaigns in the years of mission preparation, with the goal to test operational procedures and refine the algorithms for the processing chain. Experience gained with the A2D supported the ground tests conducted with ALADIN before the launch of Aeolus in 2018. It also laid the foundation for the continuous performance monitoring of the mission, performed within the Data Innovation and Science Cluster (DISC), led by DLR. After launch, DLR executed four airborne campaigns with a focus on validating the Aeolus wind products during different phases of the mission and in diverse geographical and meteorological conditions. During these campaigns, the DLR Falcon aircraft was equipped with the A2D and a high-accuracy scanning heterodyne-detection 2-µm Doppler wind lidar (DWL), used as a reference. Complementary and synergistic results from both DWLs do not only allow for the characterization of the Aeolus and A2D wind errors, but also provide recommendations for the optimization of the Aeolus wind retrieval. Fielding the A2D as a test-bed and validation tool for the Aeolus mission has been a milestone for space lidars and vital for the success of Aeolus, as it has been providing efficient access to instrument specifics in the technological, analytical and scientific domains. The paper covers selected aspects of the airborne technology demonstration program that has supported Aeolus in becoming a successful explorer mission, able to provide high impact data for numerical weather prediction institutions around the world on an operational basis.

Keywords: Aeolus, space-borne wind lidar, heterodyne-detection wind lidar, direct-detection wind lidar, validation

*christian.lemmerz@dlr.de; dlr.de/pa/en/lidar

1. INTRODUCTION

ALADIN on-board Aeolus is the first European spaceborne lidar and the first direct-detection DWL. The ESA Aeolus mission provides profiles of the wind vector component along the instrument's line-of-sight (LOS) direction from ground up to about 30 km [1]. After launch on 22 August 2018, Aeolus was injected into a sun-synchronous dusk-dawn orbit at about 320 km altitude. The lidar transmitter is operating at an ultraviolet (UV) wavelength of 354.8 nm and the receiver is designed to determine the Doppler shift of the backscattered light from both molecules and particles and hence the LOS wind speed. The backscattered light, collected by a 1.5 m diameter telescope, is first directed to a Fizeau interferometer which can analyze the frequency shift of the narrowband particulate (Mie-scattered) return signal by detecting the position of a transmitted fringe imaged on an accumulating charge–coupled device (ACCD) detector. Most of the light is rejected by the Fizeau and reflected to two sequentially coupled Fabry–Pérot interferometers. Their transmission functions are separated in frequency such that the Doppler shift of the broadband molecular (Rayleigh-scattered) return signal is determined by comparing the individual transmitted intensities, both detected with a second ACCD. Range bins can be set for a vertical resolution between 250 m and 2 km and changed along the orbit. The complex optical arrangement has proven its ability to capture the global wind fields already three weeks after launch, delivering valuable wind products converted

to the horizontal LOS (HLOS) direction, which serves as input for numerical weather prediction (NWP) models. In the following years, the Aeolus data assimilation has also demonstrated to improve NWP capabilities with remarkable impact, especially in the medium-range weather forecast [2].

To support the processor development and operational preparation of the ESA mission, for the first time, an airborne technology demonstrator was implemented with the equivalent instrument hardware in parallel. Starting in 2004, the ALADIN Airborne Demonstrator (A2D) was developed by ESA, Airbus-DS (formerly EADS Astrium) and DLR, featuring the special receiver optics including the spectrometers and detectors of the ALADIN pre-development model (PDM). A2D also consists of a frequency-stabilized UV laser, a Cassegrain telescope and the same dual-channel optical and electronical receiver design to measure wind speeds along the instrument's LOS by analyzing Mie- and Rayleigh backscatter signals [3]. The concept of airborne demonstration based on high commonality with the space hardware design was later also implemented by, e.g., NASA with the Airborne Cloud–Aerosol Transport System (ACATS) [4] as a test-bed for the CATS mission on the ISS, and more recently, in China with an airborne demonstrator for the Aerosol and Carbon Detection Lidar (ACDL) mission, which was launched in April 2022 [5]. Other airborne systems were fielded as precursor instruments for technology demonstration and mission preparation as described by Fix et al. and Tucker et al. in [6] and [7], respectively.

The new and sophisticated arrangement of spectrometers and ACCD detectors was driving the effort to develop the A2D, based on the Aeolus instrument ALADIN PDM receiver optics and electronics, to maximize technological representativity in design and measurement principle. The system has been deployed by DLR for studies in the optical laboratory as well as during various ground and airborne field campaigns since 2005. A scanning, heterodyne-detection DWL operating at 2-µm wavelength [8] acted as a reference by providing a high accuracy and sensitivity to particulate returns with the extra capability to measure wind vector profiles for the A2D and Aeolus validation. The combination of both DWLs enabled to explore the ALADIN-specific wind measurement technology of A2D under various atmospheric conditions. Both instruments were also operated in parallel on the DLR Falcon research aircraft in a downward looking configuration similar to Aeolus, to capture wind profiles from an altitude of 10 km to 11 km to the ground. Compared to Aeolus, they offer higher horizontal resolution and the possibility to directly influence and monitor all relevant system parameters. Using the 2-µm DWL as a reference, the A2D allowed us to verify and validate the complex direct-detection measurement technique for wind and aerosol, its operational limits, instrument calibration procedures, alignment sensitivity, noise characteristics and many more specifics of the instrument. With these activities, the capabilities expected for Aeolus had been demonstrated already before launch, as described in [9] and [10]. Moreover, thanks to the extensive pre-launch program, the operational experience and algorithm development for Aeolus grew to a level that paved the way for the fast commissioning and quick success of the mission after its launch in August 2018. It also formed the basis for the DLR-led Data Innovation and Science Cluster which was implemented to support the Aeolus mission with performance monitoring and processor development [11]. Besides the Aeolus performance monitoring based on the satellite data in the framework of DISC, DLR also conducted four airborne validation campaigns during the first three years of the mission. For the airborne activities the two DWLs were again installed onboard the DLR Falcon, performing coordinated underflights along the Aeolus track. After three campaigns in Central Europe and the North Atlantic region around Iceland in 2018 and 2019, DLR contributed to the Joint Aeolus Tropical Atlantic Campaign (JATAC) around Cape Verde in September 2021 [12].

The paper presents a selection of the A2D contributions supporting the Aeolus mission, where the following section describes the A2D, before providing examples of pre-launch activities and their results. The final section covers the Aeolus validation campaigns conducted for determining the Aeolus L2B wind product's systematic and random errors as well as potential improvements of the wind retrieval algorithms.

2. THE ALADIN AIRBORNE DEMONSTRATOR

The A2D wind lidar is composed of a pulsed, frequency stabilized UV laser transmitter incorporating a reference laser system, a Cassegrain telescope, a front optics arrangement, and the ALADIN-type dual-channel receiver including ACCD detectors, as described in detail in [3] and [13]. A schematic of the lidar is depicted in Figure 1. The laser transmitter is based on a Nd:YAG master-oscillator power amplifier design similar to the ALADIN lasers with second and third harmonic generation (SHG/THG) stages, for conversion to the UV output at 355 nm. As it is necessary for calibrating the spectrometer responses for ALADIN-type DWLs, the UV output is tunable over a frequency range of almost 12 GHz with a frequency-agile reference laser system used for injection-seeding of the oscillator. For maintaining the frequency stability, the oscillator cavity is of a mechanically rigid design and controlled by a modified ramp-delay-fire technique, which was developed together with Airbus-DS and the Fraunhofer Institute for Laser Technology (ILT) [14]. This concept

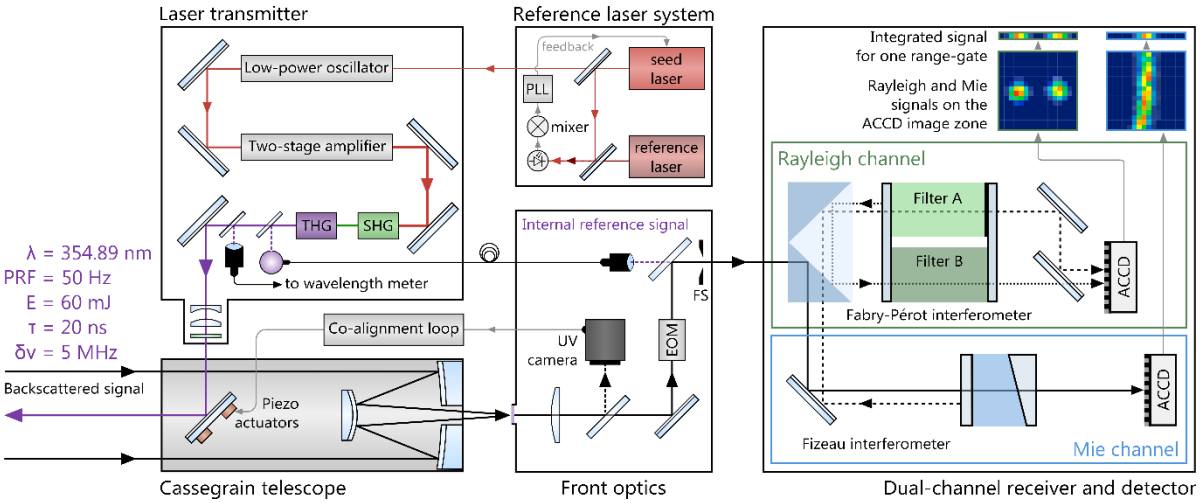

Figure 1. Schematic of the A2D principle design (modified from [13]), featuring the Mie and Rayleigh channel with the Fizeau and Fabry Pérot interferometers (FPI) and the ACCDs from the Aeolus PDM in the same configuration as on ALADIN in space. Quarter waveplate (QWP), polarizing beam splitter (PBS), electro-optic modulator (EOM), phase-locked loop (PLL), field stop (FS). For more details see text.

proved to fulfil the demanding requirements for wind measurements even in the vibrating environment of airborne operations [15]. Unlike implemented in ALADIN, the A2D laser has pick-ups for the outgoing UV pulse, delivering both a reference signal to the spectrometers via a mode-scrambled multi-mode fiber and for feeding a high-performance UV wavelength meter. The independent frequency stability measurement available from the wavelength meter was the basis for characterizing the influence of the mode-scrambling on the frequency determination capabilities of the spectrometers in the A2D [16] and for the support of ALADIN transmitter ground tests before launch [17]. The knowledge gained also allowed us to verify the frequency stability performance of Aeolus in space and its impact on the wind error as well as its sensitivity to vibrations caused by resonances with critical reaction wheel speeds, as described in Lux et al. [18].

Table 1. Specifications for ALADIN and A2D

Parameter	ALADIN on Aeolus	ALADIN Airborne Demonstrator (A2D)
Laser wavelength	354.8 nm	354.9 nm
Repetition rate	50.5 Hz	50.0 Hz
Pulse energy	53…90 mJ	60...70 mJ
Linewidth	30 MHz (FWHM)	50 MHz (FWHM)
Telescope diameter	1.5 m	0.2 m
LOS slant angle	35°	20°
Optical layout	Transceiver	Mono-static with active co-alignment
Receiver	Sequential Fabry-Pérot interferometers for molecular backscatter (Rayleigh channel) and Fizeau interferometer for particulate backscatter (Mie channel)	
Horizontal resolution	86.4 km / 10 km	3.6 km
Vertical resolution	250 m to 2000 m depending on range bin setting	300 m to 1200 m depending on range bin setting

Compared to ALADIN, which is designed in a transceiver optical arrangement based on circular polarized emission for separating the outgoing and return light paths, A2D has a co-axial layout with a co-alignment loop. This enables a more flexible modular lidar concept and also eases the step-wise A2D aircraft integration procedure. To set the circular

polarization, QWPs are inserted in the emission and reception paths. A small portion of the return signal is detected with a UV camera in the front optics to measure the position within the field-of-view (FOV). The offset to a defined reference position is fed back to piezo actuators controlling the laser beam direction in order to maintain the overlap of the emission and reception FOVs. Without the milliseconds delay for the atmospheric return experienced by Aeolus on a 320 km orbit, the A2D had to be equipped with an EOM to prevent a contamination of the internal reference signal during its acquisition by blocking the atmospheric path for a view µs. The telescope is mounted 20° off nadir in the aircraft, limited by the bottom fuselage window size, which slightly modifies the vertical resolution defined by the ACCD acquisition speed and range bin setting compared to the 35° of Aeolus. The slower aircraft speed of about 200 m/s increases the horizontal resolution to 3.6 km. Table 1 summarizes the main specifications for both ALADIN and the A2D for comparison.

3. A2D PRE-LAUNCH ACTIVITIES FOR MISSION PREPARATION

In its first years, the A2D was used to study the basic details influencing the radiometric and wind-determination performance of the ALADIN-type spectrometer arrangement, which was -for the first time- illuminated with atmospheric lidar returns. This is in many respects different from the system level instrument characterization performed during instrument development and integration. For example, the sequential implementation of Fabry-Pérot interferometers for the Rayleigh channel illuminated by the reflection of the Fizeau-Interferometer in the Mie channel was known to have a complex transmission function, which is both sensitive to alignment changes and cross-talk from narrow-band particulate return signal. Concerning the Mie channel, fringe-imaging characteristics combined with low optical throughput of the Fizeau and high SNR requirements for reliable wind were studied. The ACCD detector read-out causes a range gate overlap and thus potentially large wind biases in case of strong signal gradients like experienced with cloud and ground return. This is due to imperfections in the fringe shape and illumination on the Mie-channel and due to different response slopes for broad-band molecular and narrow-band particulate atmospheric return spectra in the Rayleigh-channel. Depending on accumulation length on the ACCD, the frequency stability of the laser has varying influence on the wind error in both channels and different for homo- and heterogenous atmospheric scenes. These topics as well as ground and sea-surface return characteristics were studied with data acquired during two ground campaigns at the observatory of the German weather service (DWD) in Lindenberg and two airborne campaigns with the DLR Falcon conducted from Oberpfaffenhofen, Germany until 2008. The airborne activities featured also the first airborne measurements of a direct-detection DWL as well as the first combined deployment of a direct- and heterodyne-detection DWL, while providing an Aeolus-like downward looking geometry and related atmospheric return characteristics. Related references to these topics and the following described in this chapter are summarized in Table 2, instead of in the text.

Table 2. Overview of pre-launch study topics performed with A2D in support of the Aeolus mission preparation

A2D Study Topic	Reference
A2D performance and influences including simulations	[15], [19], [20], [21], [22]
Sea surface return characteristic	[23]
Rayleigh-Brillouin line shape and related atmospheric temperature profile measurements	[24], [25], [26], [27], [28]
Noise characterization	[16], [29]
International airborne campaigns covering performance issues associated with strong wind speeds, wind and signal gradients, various atmospheric and albedo scenes as well as calibration and satellite validation strategies	[30], [31], [32], [33], [34], [35]
Aerosol retrieval	[36]

In 2009, the A2D was set-up on the Alpine observatory Schneefernerhaus, situated on the Zugspitze mountain to verify the Rayleigh-Brillouin line-shape in air and its influence of the on the Fabry-Pérot interferometer transmission. For the first time, this study confirmed the Rayleigh-Brillouin scattering characteristics in the atmosphere and the importance of its consideration in the Rayleigh channel wind retrieval. It also led to a simplified analytical model valid for the Aeolus-relevant atmospheric domain. These results later also allowed to measure temperature profiles with a lidar from ground and airborne during daylight conditions, as demonstrated with the A2D in the following years for the first time. The set-up on the mountain observatory was also used for extensive hard-target measurements at full-overlap ranges including alignment sensitivity measurements. Overall, this provided the detailed understanding which is the basis for the Aeolus in-

flight spectral performance monitoring mentioned in section 4.2. The 3rd pre-launch airborne campaign was conducted in the North-Atlantic region around Iceland and Greenland in autumn of 2009, with the goal to capture strong wind speeds and wind gradients along various atmospheric, solar background and ground albedo scenes. Analysis of this data not only allowed us to test and refine the processor suite developed for Aeolus, but also delivered input for the Aeolus End-to-End Simulator (E2S) and finally led to an intensive study of the different noise contributions with the A2D from 2013.

Two major airborne campaigns (WindVal-I and -II) with international contributions were carried out in 2015 and 2016, again in the North-Atlantic region with a base in Iceland. These campaigns focused on extending the dataset acquired during the previous airborne campaigns with respect to wind measurements and A2D calibrations in various conditions. Additional active, passive and in-situ instruments on the partnering research aircraft provided both various measurements for wind comparison, including lidar and radar results, and complementary data like e.g. temperature profiles from dropsondes. Among the goals of these campaigns was to develop and test satellite validation strategies for Aeolus, practiced with underflights of the TDS (TechDemoSat) and ASCAT (Advanced SCATterometer) satellite instruments, as shown in Figure 2. With this, these campaigns were not only condensing the community which finally led to the international airborne Aeolus validation effort covered in the following section, but also contributed to positive public outreach across Europe and the US. Scientific results provided the basis for the quick success of the Aeolus mission after launch by proving the measurement principle and its performance based on subsequently refined processing algorithms. The potential to meet the demanding performance requirements and limitations of the ALADIN concept were revealed.

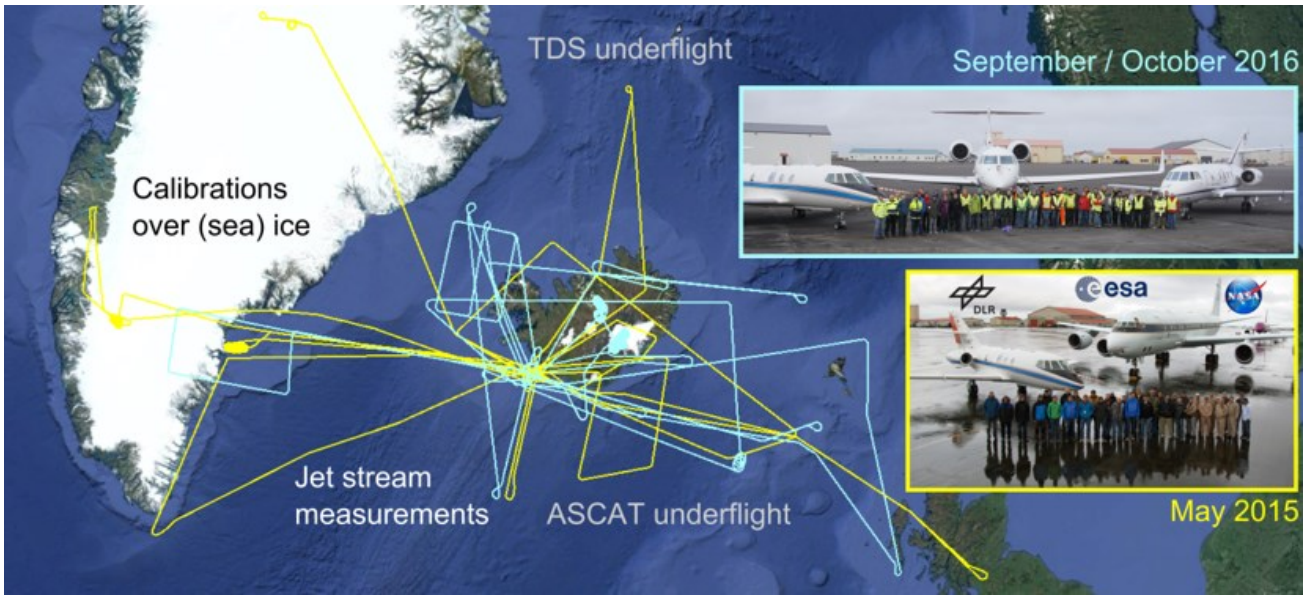

Figure 2. Flight tracks and objectives of the DLR Falcon equipped with the A2D and 2-µm DWLs during the WindVal campaign in 2015 (yellow tracks) and during WindVal-II/NAWDEX in 2016 (light blue). The inserts show the international contribution from campaign partners of the DLR Falcon, featuring the NASA DC-8 in 2015 and the French Falcon together with the German HALO in 2016.

4. AEOLUS VALIDATION AND PERFORMANCE MONITORING

The experience gained from operating the A2D supported the evaluation of ground tests that were performed with Aeolus before launch, both as an instrument full performance verification at ambient conditions and a thermal vacuum test simulating space environment. It also led to duties for the continuous monitoring of the Aeolus instrument performance within the DISC after launch. In parallel, an extensive airborne validation program was conducted to assess the quality of the Aeolus wind products and to support the further refinement of the processing chain.

4.1 DLR Aeolus Validation Campaigns Overview

Based on the lessons learned from the pre-launch campaigns, DLR conducted the first Aeolus airborne validation campaign WindVal-III already during the commissioning phase in late 2018. Off the base in Oberpfaffenhofen four flights were conducted along ascending orbits in the evening hours. This campaign was followed by a second campaign in central

Europe, again conducted from Oberpfaffenhofen, which started a series of validation campaigns during the operational phase of the Aeolus mission. AVATAR-E (Aeolus Validation Through Airborne LidaRs in Europe) was covering six underflights again on ascending orbits, but in the late phase of the active period of laser A with decreased performance in spring of 2019. In the autumn of the same year, after the laser B had been commissioned, the artic and North Atlantic region was targeted from a base in Keflavík, Iceland for the AVATAR-I campaign. The total of ten underflights also include four flights on descending orbits (performed in the early morning hours) as well as flights along the high-albedo, snow-covered east coast of Greenland. A main focus lied again on capturing the strong wind speeds and gradients associated with the polar jet stream in this region. A dedicated range bin setting (RBS) for Aeolus supported this goal, by providing higher vertical resolution within the campaign area. Delayed by more than one year due to COVID-19 related logistical issues, the Tropical region was the scene for the AVATAR-T campaign in autumn of 2021. Five descending and six ascending orbit underflights were conducted with a focus on the specific atmospheric conditions influenced by strong Saharan dust outbreaks and the African Easterly Jet (AEJ) winds around the Cape Verdean archipelago. With a base in Sal this campaign was embedded in the Joint Aeolus Tropical Atlantic Campaign (JATAC) together with ESA, NASA, the French CNES/LATMOS and other European partners. JATAC was carried out with contributions from the NASA DC-8, the German and French Falcons and a strong ground-based and light aircraft component organized by the National Observatory of Athens (NOA) and TROPOS, offering a wide range of in-situ as well as active and passive remote sensing measurement equipment [37]. A dedicated RBS was active in the region during JATAC to ensure a high resolution in the middle to lower troposphere and the AEJ. During all campaigns, additional calibration flights were conducted for the A2D where the aircraft is rolled 20° to the right and circles an area, while the lidar is pointing nadir to justify the assumption of zero wind influence on the LOS during the performed frequency sweep to characterize the spectrometer responses [33]. An overview of the campaign flights is given in Figure 3 together with a table of the campaign statistics.

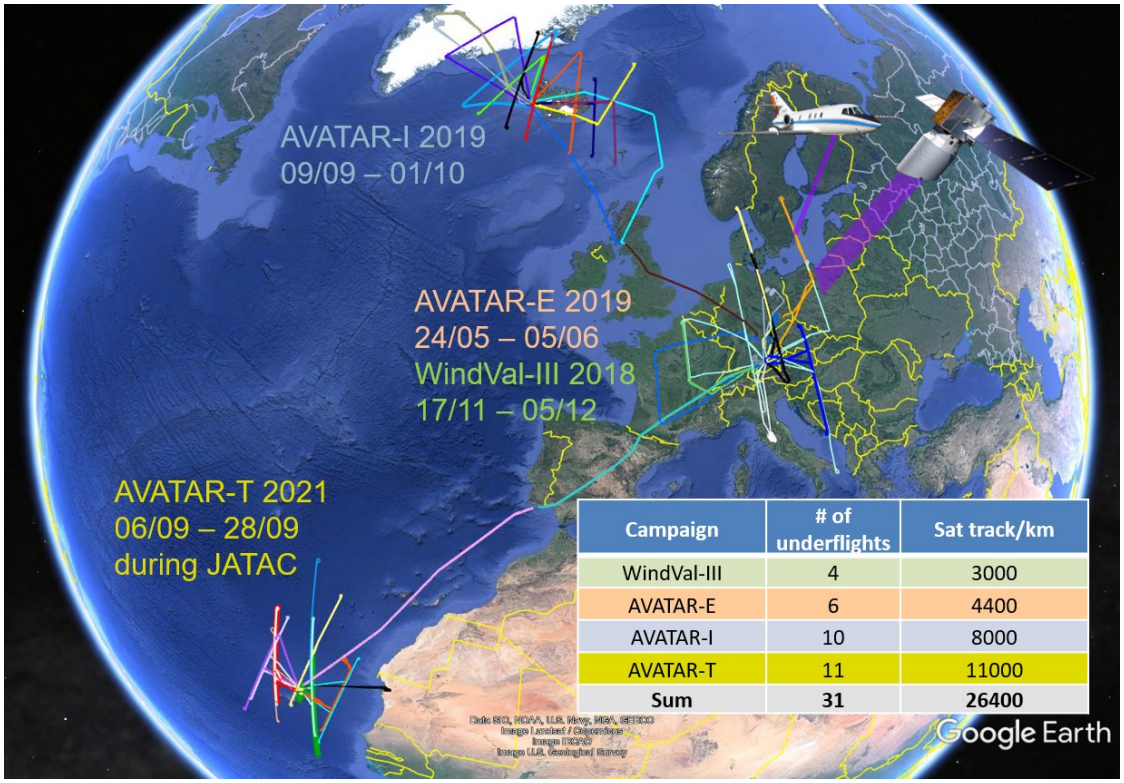

Campaign	# of underflights	Sat track/km
WindVal-III	4	3000
AVATAR-E	6	4400
AVATAR-I	10	8000
AVATAR-T	11	11000
Sum	**31**	**26400**

Figure 3. Overview of the four DLR airborne campaigns with their flight tracks performed for the Aeolus validation in different mission phases and locations (background image © 2022 Google). The insert table summarizes the campaign statistics with the number of satellite underflights.

Individual flights and whole campaign datasets provide an intermediate validation perspective between the local validation with ground sites and the more global perspective of NWP-based validation strategies. Collocated airborne measurements also ensure a high representativity with a time difference to the overpass of usually not more than 45 minutes. For Aeolus this allows us to study the influence of different atmospheric scenes on the performance of the Mie and Rayleigh channel

wind products in terms of coverage and error distribution. As an example, results from an approximately 900 km long flight leg performed along an ascending orbit during the AVATAR-T campaign are shown in Figure 4. Since the Aeolus L2B Rayleigh-clear and Mie-cloudy products as well as the ECMWF model background winds are provided for the HLOS direction (see right column), the airborne lidar wind measurements also have to be converted to this satellite viewing direction while considering the wind nomenclature (positive winds blowing away from the instrument) for the statistical comparison. Figure 4 shows the finer resolution for the measured airborne data in the left column, which provides insights into errors in the Aeolus data products stemming from vertical or horizontal atmospheric inhomogeneities. The right column reveals the different coverage of the Aeolus Rayleigh and Mie channel in the dust layers below 6 km compared to the respective A2D results, which initiated an ongoing study.

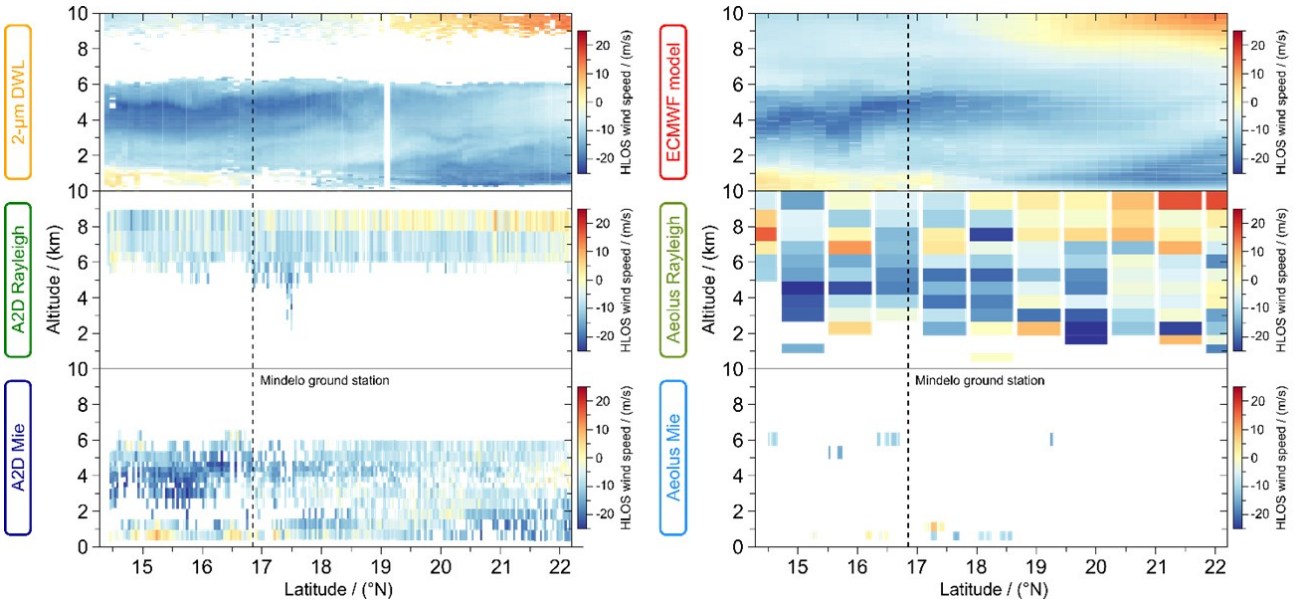

Figure 4. Example of the wind data products for an Aeolus validation flight on Friday, 10 September 2021 passing the ground measurement site in Mindelo. 2-µm measurements and the ECMWF model winds are shown in the upper row with Rayleigh and Mie channel winds measured by the A2D (left) and Aeolus (right) below, all shown for the HLOS wind component.

Focusing on the wind data of the 2-µm DWL in Figure 4, it is clear that the signal coverage of the heterodyne system is limited to the first 1 km below the aircraft and the dust-laden Saharan Air Layer (SAL). Within the SAL detailed structures of the AEJ are revealed with horizontal wind speeds of up to 20 m/s. In comparison, the ECMWF model winds partly show deficiencies in correctly representing the AEJ position and strength. The A2D Rayleigh winds provide good coverage in the aerosol-free regions, while the Mie channel covers the winds within the SAL and down to the surface. The importance of the winds in clear atmosphere and the abundance of aerosol-free regions in weather-relevant altitudes around the globe were the main drivers to justify the UV wavelength and spectrometer arrangement of Aeolus (and thus A2D), although the Mie channel has a lower sensitivity compared to the heterodyne detection of the 2-µm DWL. The Aeolus Mie-cloudy product in this scene only provides very few valid wind results, as the processors are not optimized for the strong aerosol scattering case within the SAL. This aerosol scattering still provides lower signal-to-noise ratios than in case of particulate return from most of the cloudy scenes. A2D results suggest that a refinement of the Aeolus processor could lead to enabling a “Mie-aerosol“ wind product as well as to a more effective rejection of detrimental particulate return signals that affect the Rayleigh-clear winds. In principle, the quality of Rayleigh winds detected in these dust regions can be decreased by both this so-called channel cross-talk and the signal attenuation within the SAL. The same is true for winds that are measured within and/or below similar layers of aerosol or thin clouds around the globe.

For the statistical comparison, the airborne data is averaged to the coarser vertical and horizontal resolution of the Aeolus measurement grid. The procedures applied for the statistical comparison with the airborne DWL data and results of the systematic and random errors in both Aeolus channels are described in detail by Witschas et al. and Lux et al. for the first two campaigns in [38] and [39], as well as in [40] and [41], respectively, covering also the two later campaigns. The best Aeolus performance was observed in the frame of the AVATAR-I campaign which took place during the early laser B

period in autumn 2019. Here, comparison of the Aeolus winds against 2-µm DWL data yielded random errors (in terms of the scaled median absolute deviation) of 3.8 m/s for Rayleigh-clear winds during ascending orbits, and 2.3 m/s for the Mie-cloudy winds during descending orbits, respectively. Both values were obtained after averaging to a vertical bin thickness of 1 km.

4.2 Aeolus performance monitoring and mission support

From the intensive monitoring and mission support organized within the DISC, this article has to focus on a small selection of examples with reference to the A2D. Besides the frequency monitoring based on pulse-to-pulse Mie channel measurement of the internal reference signal and its results mentioned in section 2, the internal reference signal of both channels was also used to monitor the spectral performance of the spectrometers, as it was also regularly executed during A2D operations by tuning the reference laser frequency over one free spectral range of the FPI. Figure 5 (a) shows the detailed transmission functions of the Rayleigh spectrometer including the reflection function of the optically up-stream Fizeau spectrometer and their evolution. The direct (left peak) and reflected (right peak) Fabry-Pérot channels correspond to FPI A and B, respectively, in Figure 1. Keeping the normalized frequency referenced to the maximum transmission of the direct channel, it is revealed that the reflected channel maximum transmission and the frequency spacing both drift during the laser flight model A (FM-A) initial period after the Aeolus launch. Such a behavior has been observed before with the A2D depending on the input angle alignment and/or illumination pattern. The spectral drifts lead to changes in the frequency response of the Rayleigh channel affecting both the error in wind and aerosol products, thus confirming the need for regular calibrations. A detailed analysis covering also the FM-B period was published by Witschas et al. in [42].

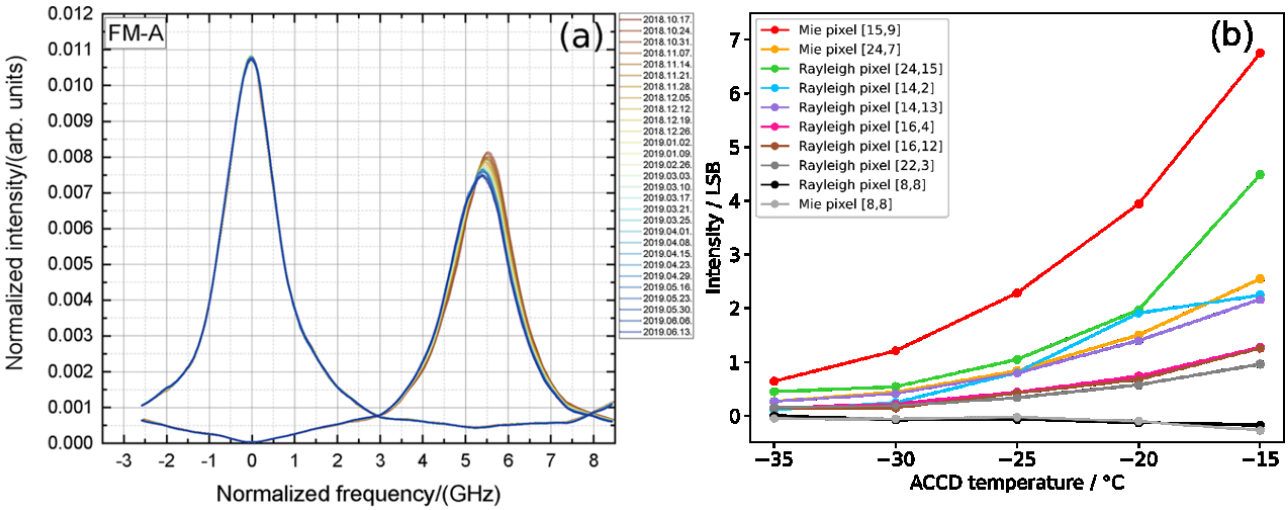

Figure 5. Examples for Aeolus mission support based on A2D experience. On the left side (a) the evolution of the Aeolus Fabry-Pérot transmission functions during the laser A phase after Aeolus launch is shown (extracted from [42]). (b) shows the temperature sensitivity of the noise level (in units of least significant bits, LSB) associated to a view detected suspicious pixels in the ACCD accumulation zone of the A2D.

Figure 5 (b) shows the result of a dedicated measurement performed with the A2D in the lab to screen the ACCD in all modes for suspicious pixels and their activation dependence on the ACCD temperature. This was done after identifying an increasing number of so-called “hot” pixels in both channels over the course of the Aeolus mission, which irregularly cause strong biases after their spontaneous activation. With the ACCDs implemented in the A2D being the only readily available samples that can be operated and controlled in temperature, dedicated tests were performed in the DLR optical laboratory to support investigations on the root cause and possible mitigation strategies. As for the A2D ACCDs, no hot pixels were detected, supposedly due to the non-space environment and/or limited duty time compared to the 24/7 operation on Aeolus. However, “lukewarm” pixels could be identified, but with activation intensities irrelevant for typical A2D intensities acquired during measurements. The determined temperature sensitivity characteristics suggest to both consider lower operating temperatures for the implementation of similar technology detectors in future space missions like an Aeolus follow-on DWL and to repeat the test procedure if possible on ALADIN, which is currently investigated as a test to be executed towards the end of the Aeolus mission. To mitigate the hot-pixel-induced bias for Aeolus, dedicated dark current

measurements were introduced in sufficient cadence as a monitoring strategy. Based on these measurements the hot pixel intensities are corrected for in the background signal treatment, as discussed by Weiler et al. in [43].

5. SUMMARY AND OUTLOOK

Thanks to the high degree of commonality with the satellite instrument in terms of design and measurement principle, the experience gained from operating the A2D already during the Aeolus mission preparation was crucial for clarifying and mitigating issues that were relevant for the performance and operations, well before launch. The in-depth investigations performed in the frame of dedicated airborne and ground measurement campaigns gave insight into ALADIN-specific details that were not visible, investigated or detected during sub-system as well as instrument full performance tests done throughout the satellite development and integration phases. This is especially true for the impact of atmospheric signal characteristics on the wind measurement performance of the sequential spectrometer arrangement. With wind vector profiles provided by the heterodyne-detection 2-µm DWL operated in parallel to the A2D, it could be demonstrated that the ALADIN-type direct-detection instrument can in principle meet the performance requirements stated for Aeolus.

Well above 100 recommendations for the mission were derived from A2D activities, covering issues on instrument alignment, operation, retrieval algorithms, calibration and validation as well as input for the E2S development and refinement. This work supported ESA and space industry already during the ground tests and fostered the quick success of Aeolus after launch. The knowledge generated with the A2D left only a few unexpected Aeolus-specific issues arising during the mission, which could be quickly identified and solved by the experienced DISC community. After launch, more than 26,000 km of collocated A2D and 2-µm wind observations were acquired along the Aeolus track during four airborne campaigns. These were performed in different geographical regions and under diverse atmospheric and solar background conditions, while being distributed along the Aeolus performance evolution. The data collected during these campaigns provide valuable information for the optimization of the Aeolus wind retrieval and related quality control algorithms. Algorithm improvements developed for the A2D wind retrieval contribute to the enhancement of the Aeolus products and their quality. Thus, the campaign data will continue to be relevant for testing re-processed Aeolus products and also foster the derivation of new secondary mission products.

A2D heritage and dedicated measurements during the mission phase have been supporting Aeolus by performing detailed instrument monitoring based on the available satellite housekeeping data, and by providing a test-bed for analyzing unexpected issues like the ALADIN-specific hot-pixels. Altogether, the implementation and continuous utilization of the A2D delivered significant value for the Aeolus mission and all involved parties, despite being based on a comparably small funding line, which has been cooperatively organized by DLR and ESA. The airborne technology investigations and demonstration increased the Aeolus program efficiency by complementing and extending tests performed within ESA and the space industry. It has provided feedback with detailed holistic system knowledge and support for securing the mission success whenever required. Meanwhile, the A2D is being further developed towards a 2nd generation instrument with a 100 Hz UV laser. The versatile instrument set-up allows for considering design modifications like the implementation of a cross-polar channel in linear or circular polarization configuration and the test of different spectrometer or detector concepts. The next generation of an airborne heterodyne-detection DWL as a reference is also in development. It is highlighted that a further successful mission support for a potential Aeolus follow-on DWL candidate can be founded on this heritage and an accordingly modified 2nd generation A2D.

Funding:

The discussed activities were successive projects over the years, funded by both DLR and ESA.

Acknowledgements:

The great support and professionality of the DLR Flight Experiments Facility in conducting the flight campaigns with the DLR Falcon always considering the special requests and scientific needs were an integral part of the successful airborne demonstration. Highly acknowledged is also the continuous contribution by Engelbert Nagel, who helped realizing the demanding projects with dedication in all technical aspects.

REFERENCES

[1] European Space Agency (ESA), "ADM-Aeolus Science Report," ESA SP-1311, 121 p., https://earth.esa.int/documents/10174/1590943/AEOL002.pdf (2008).

[2] M. P. Rennie, L. Isaksen, F. Weiler, J. Kloe, T. Kanitz and O. Reitebuch, "The impact of Aeolus wind retrievals in ECMWF global weather forecasts," Q. J. R. Meteorol. Soc., https://doi.org/10.1002/qj.4142 (2021).

[3] O. Reitebuch, C. Lemmerz, E. Nagel, U. Paffrath, Y. Durand, M. Endemann, F. Fabre and M. Chaloupy, "The Airborne Demonstrator for the Direct-Detection Doppler Wind Lidar ALADIN on ADM-Aeolus. Part I: Instrument Design and Comparison to Satellite Instrument," J. Atmos. Oceanic Technol., 26, 2501–2515, https://doi.org/10.1175/2009JTECHA1309.1 (2009).

[4] Yorks, J. E., et al., "The Airborne Cloud-Aerosol Transport System: Overview and Description of the Instrument and Retrieval Algorithms," J. Atmos. Oceanic Technol., 31 2482 –2497, https://doi.org/10.1175/JTECH-D-14-00044.1 (2014).

[5] Ke, J., et al., "Development of China's first space-borne high-spectral-resolution lidar: retrieval algorithm and airborne demonstration," PhotoniX, 3(1), 1-20, (2022).

[6] Fix, A., Amediek, A., Ehret, G., Groß, S., Kiemle, C., Reitebuch, O. and Wirth, M., "On the benefit of airborne demonstrators for space borne lidar missions," In International Conference on Space Optics—ICSO 2016 (Vol. 10562, pp. 541-549). SPIE (2016)

[7] Tucker, S. C., Weimer, C. S., Baidar, S. and Hardesty, R. M., „The optical autocovariance wind lidar. Part I: OAWL instrument development and demonstration," Journal of Atmospheric and Oceanic Technology, 35(10), 2079-2097 (2018)

[8] Witschas, B., Rahm, S., Dörnbrack, A., Wagner, J. and Rapp, M., "Airborne Wind Lidar Measurements of Vertical and Horizontal Winds for the Investigation of Orographically Induced Gravity Waves," J. Atmos. Ocean. Tech., 34, 1371–1386, https://doi.org/10.1175/JTECH-D-17-0021.1 (2017)

[9] Marksteiner, U., Lemmerz, C., Lux, O., Rahm, S., Schäfler, A., Witschas, B. and Reitebuch, O., "Calibrations and Wind Observations of an Airborne Direct-Detection Wind LiDAR Supporting ESA's Aeolus Mission," Remote Sensing, 10, 2056 (2018).

[10] Lux, O., Lemmerz, C., Weiler, F., Marksteiner, U., Witschas, B., Rahm, S., Schäfler, A. and O. Reitebuch, "Airborne wind lidar observations over the North Atlantic in 2016 for the pre-launch validation of the satellite mission Aeolus," Atmos. Meas. Tech., 11, 3297–3322 (2018).

[11] Reitebuch, O., "Contributions from the DISC to accomplish the Aeolus mission objectives," Taormina, Italy, 28 March – 1 April 2022, https://www.aeolus3years.org/detailed-agenda (last access: 20 August 2022) (2022)

[12] Skofronick-Jackson, G., Fehr, T., et al., "The Joint Aeolus Tropical Atlantic Campaign - First Results for Aeolus Calibration/Validation and Science in the Tropics," ATMOS 2021, ESA (2021).

[13] Lux, O., Lemmerz, C., Weiler, F., Marksteiner, U., Witschas, B., Rahm, S., Schäfler, A. and Reitebuch, O., "Airborne wind lidar observations over the North Atlantic in 2016 for the pre-launch validation of the satellite mission Aeolus," Atmospheric Measurement Techniques, 11(6), 3297-3322 (2018).

[14] Nicklaus, K., Morasch, V., Hoefer, M., Luttmann, J., Vierkötter, M., Ostermeyer, M., Lemmerz. C. and Hoffmann, D., "Frequency stabilization of Q-switched Nd: YAG oscillators for airborne and spaceborne lidar systems," In Solid State Lasers XVI: Technology and Devices (Vol. 6451, pp. 387-398). SPIE (2007).

[15] Lemmerz, C., Lux, O., Reitebuch, O., Witschas, B., & Wührer, C., "Frequency and timing stability of an airborne injection-seeded Nd: YAG laser system for direct-detection wind lidar," Applied Optics, 56(32), 9057-9068 (2017).

[16] Lux, O., Lemmerz, C., Weiler, F., Marksteiner, U., Witschas, B., Nagel, E. and Reitebuch, O., "Speckle Noise Reduction by Fiber Scrambling for Improving the Measurement Precision of an Airborne Wind Lidar System," In 2019 Conference on Lasers and Electro-Optics Europe & European Quantum Electronics Conference (CLEO/Europe-EQEC) (pp. 1-1), IEEE (2019).

[17] Mondin, L. and Bravetti, P., "Aeolus high energy UV Laser wavelength measurement and frequency stability analysis," In International Conference on Space Optics—ICSO 2014 (Vol. 10563, pp. 952-958), SPIE (2017).

[18] Lux, O., Lemmerz, C., Weiler, F., Kanitz, T., Wernham, D., Rodrigues, G., ... & Reitebuch, O. (2021). ALADIN laser frequency stability and its impact on the Aeolus wind error. Atmospheric Measurement Techniques, 14(9), 6305-6333.

[19] Paffrath, U., Lemmerz, C., Reitebuch, O., Witschas, B., Nikolaus, I. and Freudenthaler, V., "The airborne demonstrator for the direct-detection Doppler wind lidar ALADIN on ADM-Aeolus. Part II: Simulations and Rayleigh Receiver Radiometric performance," Journal of Atmospheric and Oceanic Technology, 26(12), 2516-2530 (2009).

[20] Reitebuch, O., Endemann, M., Engelbart, D., Freudenthaler, V., Lehmann, V., Lemmerz, C., Nagel, E., Paffrath, U., Rahm, S. and Witschas, B., "Pre-Launch Validation of ADM-Aeolus with an airborne direct-detection wind lidar," Reviewed and Revised Papers of 24th Int. Laser Radar Conf., Boulder, CO, USA, 41-44 (2008).

[21] Reitebuch, O., Paffrath, U. and Nikolaus, I., "ADM-Aeolus Ground Campaigns Results," Technical note, DLR. 26/02/2010 (2010).

[22] Reitebuch, O., Marksteiner, U. and Lemmerz, C., „ADM-Aeolus Airborne Campaigns Results," Technical note, DLR. 24/02/2012 (2012).

[23] Li, Z., Lemmerz, C., Paffrath, U., Reitebuch, O. and Witschas, B., "Airborne Lidar Experimental Measurement of the Sea Surface Reflectance," Proc. 25th ILRC (2010).

[24] Witschas, B., "Analytical model for Rayleigh–Brillouin line shapes in air," Applied optics, 50(3), 267-270 (2011).

[25] Witschas, B., "Analytical model for Rayleigh–Brillouin line shapes in air: errata," Applied optics, 50(29), 5758-5758 (2011).

[26] Witschas, B., Lemmerz, C. and Reitebuch, O., "Horizontal lidar measurements for the proof of spontaneous Rayleigh–Brillouin scattering in the atmosphere," Applied Optics, 51(25), 6207-6219 (2012).

[27] Witschas, B., Lemmerz, C. and Reitebuch, O., "Daytime measurements of atmospheric temperature profiles (2–15 km) by lidar utilizing Rayleigh–Brillouin scattering. Optics letters, 39(7), 1972-1975 (2014).

[28] Witschas, B., Lemmerz, C., Lux, O., Marksteiner, U., Reitebuch, O. and Schäfler, A., „Airborne temperature profiling in the troposphere during daytime by lidar utilizing Rayleigh–Brillouin scattering," Optics letters, 46(17), 4132-4135 (2021).

[29] Deutsches Zentrum für Luft- und Raumfahrt e.V. (DLR), „Final Report: Analysis of enhanced noise in A2D observations," AE.FR.DLR.A2D.CN11.110716, V 2.0, 110 pp. (2016).

[30] Marksteiner, U., Reitebuch, O., Rahm, S., Nikolaus, I., Lemmerz, C. and Witschas, B., "Airborne direct-detection and coherent wind lidar measurements along the east coast of Greenland in 2009 supporting ESA's Aeolus mission," Proc. SPIE, 8182, 81820J, https://doi.org/10.1117/12.897528 (2011)

[31] Marksteiner, U., "Airborne Wind Lidar Observations for the Validation of the ADM-Aeolus Instrument, "PhD thesis, Technische Universität München, 180 pp., available at: http://mediatum.ub.tum.de?id=1136781 (last access: 11 August 2022) (2013).

[32] Marksteiner, U., Reitebuch, O., Lemmerz, C., Lux, O., Rahm, S., Witschas, B., Schäfler, A., Emmitt, D., Greco, S., Kavaya, M. J., Gentry, B., Neely III, B. R., Kendall, E. and Schüttemeyer, D., "Airborne Direct-Detection and Coherent Wind Lidar Measurements over the North Atlantic in 2015 Supporting ESA's Aeolus Mission," Proc. 28th International Laser-Radar Conference, Bucharest, Romania, 25–30 June (2017).

[33] Marksteiner U, Lemmerz C, Lux O, Rahm S, Schäfler A, Witschas B. and Reitebuch O., "Calibrations and Wind Observations of an Airborne Direct-Detection Wind LiDAR Supporting ESA's Aeolus Mission," Remote Sensing, 10(12):2056, https://doi.org/10.3390/rs10122056 (2018).

[34] Reitebuch, O., Lemmerz, C., Lux, O., Marksteiner, U., Witschas, B. and Neely, R. R., " WindVal: Joint DLR-ESA-NASA wind validation for Aeolus," ESA Final Rep. 4000114053/15/NL/FF/gp, 146 pp., https://earth.esa.int/eogateway/search?text=windval&category=Document+library (2017).

[35] Lux, O., Lemmerz, C., Weiler, F., Marksteiner, U., Witschas, B., Rahm, S., Schäfler, A. and Reitebuch, O., "Airborne wind lidar observations over the North Atlantic in 2016 for the pre-launch validation of the satellite mission Aeolus," Atmos. Meas. Tech. 11, 3297–3322 (2018).

[36] Geiß, A., Marksteiner, U., Lux, O., Lemmerz, C., Reitebuch, O., Kanitz, T. and Straume-Lindner, A. G., "Retrieval of atmospheric backscatter and extinction profiles with the aladin airborne demonstrator (A2D)," In EPJ Web of Conferences (Vol. 176, p. 02021), EDP Sciences (2018).

[37] Skofronick-Jackson, G., Fehr, T., Althausen, D., Amiridis, V., Baars, H., et al., "The Joint Aeolus Tropical Atlantic Campaign - First Results for Aeolus Calibration/Validation and Science in the Tropics", ATMOS 2021, ESA (2021).

[38] Witschas, B., Lemmerz, C., Geiß, A., Lux, O., Marksteiner, U., Rahm, S., Reitebuch, O. and Weiler, F., "First validation of Aeolus wind observations by airborne Doppler wind lidar measurements," Atmos. Meas. Tech., 13, 2381–2396 (2020).

[39] O. Lux, C. Lemmerz, F. Weiler, U. Marksteiner, B. Witschas, S. Rahm, A. Geiß and O. Reitebuch, "Intercomparison of wind observations from the European Space Agency's Aeolus satellite mission and the ALADIN Airborne Demonstrator," Atmos. Meas. Tech., 13, 2075–2097 (2020).

[40] Witschas, B., Lemmerz, C., Geiß, A., Lux, O., Marksteiner, U., Rahm, S., Reitebuch, O. and Weiler, F., "Validation of the Aeolus L2B wind product with airborne wind lidar measurements in the polar North Atlantic region and in the tropics," Atmos. Meas. Tech. Discussions (2022)

[41] Lux, O., Witschas, B., Geiß, A., Lemmerz, C., Weiler, F., Marksteiner, U., Rahm, S., Schäfler, A. and Reitebuch, O., "Quality control and error assessment of the Aeolus L2B wind results from the Joint Aeolus Tropical Atlantic Campaign," Atmos. Meas. Tech. Discussions (2022)

[42] Witschas, B., Lemmerz, C., Lux, O., Marksteiner, U., Reitebuch, O., Weiler, F., Fabre, F., Dabas A., Flament T., Huber, D. and Vaughan, M., "Spectral performance analysis of the Aeolus Fabry–Pérot and Fizeau interferometers during the first years of operation," Atmospheric Measurement Techniques, 15(5), 1465-1489 (2022).

[43] Weiler, F., Kanitz, T., Wernham, D., Rennie, M., Huber, D., Schillinger, M., Saint-Pe, O., Bell R., Parrinello, T. and Reitebuch, O., "Characterization of dark current signal measurements of the ACCDs used on board the Aeolus satellite," Atmospheric Measurement Techniques, 14(7), 5153-5177 (2021).